$AgIO_4$ nanoparticles decorated on $SrTiO_3$ microspheres as a novel Z-scheme composite photocatalyst for efficient solar-driven degradation of cefixime

Khar-Lok Lim[1], *Jin-Chung* Sin[1,2*], and *Honghu* Zeng[2]

[1]Faculty of Engineering and Green Technology (FEGT), Universiti Tunku Abdul Rahman, 31900 Kampar, Perak, Malaysia
[2]College of Environmental Science and Engineering, Guilin University of Technology, Guilin 541004, China

Abstract. The presence of antibiotics in water bodies poses severe environmental and health risks, necessitating the development of efficient and sustainable remediation technologies. In this context, photocatalysis emerged as a promising approach, leveraging light energy to degrade organic pollutants. This study introduced a novel Z-scheme $SrTiO_3/AgIO_4$ composite synthesized via a solvothermal-sonochemical route, which aimed to enhance the photocatalytic degradation of cefixime under simulated sunlight. Characterization techniques such as field-emission scanning electron microscopy (FESEM), X-ray diffraction (XRD), fourier-transform infrared spectroscopy (FTIR), UV-vis diffuse reflectance spectroscopy (DRS), electrochemical impedance spectroscopy (EIS) and transient photocurrent response (TPR) were employed to elucidate the physicochemical and optoelectronic properties of the as-synthesized composite. The $SrTiO_3/AgIO_4$ composite degraded 73.8% cefixime in 120 min, which was remarkably higher compared to its individual components. The enhanced photoactivity was credited to the synergistic interplay of both semiconductors within the Z-scheme heterojunction, which promoted effective charge separation and reduced electron-hole pair recombination.

1 Introduction

Amid mounting environmental concerns, the prevalent use of antibiotics in medical and agricultural practices has attracted increased scrutiny due to their persistent nature and potential adverse effects on both ecosystems and human health. Cefixime (CFX), a third-generation cephalosporin antibiotic intended for oral administration, is effective against mild to moderate bacterial infections [1]. Nevertheless, approximately 40 to 50% of consumed CFX remains unmetabolized, with the majority subsequently discharged into various environmental settings - from rivers to hospital effluents [2]. The enduring presence and ongoing biological activity of CFX in these water sources urgently call for the development

*Corresponding author: sinjc@utar.edu.my

of more sophisticated water treatment technologies. Conventional treatment methods including physical, chemical, and biological processes, while established, often prove costly and are inefficient at removing low concentrations of pollutants [3]. Against this backdrop, photocatalysis stands out as a highly promising and sustainable solution, acclaimed for its high efficiency, low operational cost and minimal environmental footprint [4].

Over the past few years, ABX_3 perovskite-type nanomaterials have captured significant scientific interest as multifunctional materials due to their diverse optical, piezoelectric, ferroelectric, ferromagnetic and semiconducting characteristics [5]. Strontium titanate ($SrTiO_3$) is particularly notable within this group for its outstanding photochemical properties, cost-effectiveness and ease of synthesis [6]. However, the practical application of $SrTiO_3$ is constrained primarily by its reliance on UV light and swift recombination of photogenerated electron-hole pairs due to its wide bandgap [7]. To overcome these limitations, coupling $SrTiO_3$ with other materials, such as silver periodate ($AgIO_4$) offers a promising solution. $AgIO_4$, featuring highly insoluble yellow nanoparticles, a tetragonal crystal structure, and a narrow bandgap of 2.1 eV, is anticipated to markedly boost pollutant degradation due to its stability, non-toxic nature, and rapid generation of electron-hole pairs [8]. The formation of a heterojunction between $SrTiO_3$ and $AgIO_4$ results in a composite that benefits from the synergistic attributes of both materials, substantially widening their light absorption across much of the visible spectrum and thus enhancing overall photocatalytic efficiency.

In this study, a novel Z-scheme $SrTiO_3/AgIO_4$ composite was fabricated via a solvothermal-sonochemical route for the first time. The synthesized photocatalysts were comprehensively characterized using a suite of analytical techniques including field emission scanning electron microscopy (FESEM), energy dispersive X-Ray (EDX), X-ray diffraction (XRD), fourier-transform infrared spectroscopy (FTIR), UV-vis diffuse reflectance spectroscopy (DRS), electrochemical impedance spectroscopy (EIS) and transient photocurrent response (TPR). The photocatalytic performance of $SrTiO_3/AgIO_4$ composite was evaluated by its ability to degrade cefixime under simulated solar irradiation. As far as we are aware, this study is the first of its kind to report the photodegradation of cefixime using the Z-scheme $SrTiO_3/AgIO_4$ composite. This work is anticipated to set the precedent in exploring the catalytic properties, photocatalytic performance and mechanism of the $SrTiO_3/AgIO_4$ composite on CFX degradation.

2 Materials and methods

Ethanol (C_2H_5OH, 99.7%), ethylene glycol (EG, 99.5%), silver nitrate ($AgNO_3$, 99%) and strontium nitrate ($Sr(NO_3)_2$, 99%) were procured from R&M Chemicals. Cefixime (CFX, 98%) and sodium hydroxide (NaOH, 98%) were acquired from Acros Organics. Sodium metaperiodate ($NaIO_4$, 99%) and titanium butoxide (TBT, 97%) were purchased from Sigma-Aldrich.

For the preparation of $SrTiO_3$, TBT (5 mmol) was first dispersed in EG-deionized water mixture. Then, $Sr(NO_3)_2$ (10 mL, 0.5 M) and NaOH (5 mL, 5 M) were separately added to the TBT mixture under continuous stirring. The resulting mixture was poured into an autoclave and heated at 160°C for 24 h. The obtained precipitate was thoroughly washed at least 3 times with C_2H_5OH and deionized water, and finally dried at 60°C for 12 h. The $SrTiO_3/AgIO_4$ composite was synthesized by dispersing 0.5 g of $SrTiO_3$ in the aqueous solution containing a measured amount of $AgNO_3$. Afterward, $NaIO_4$ with Ag:I molar ratio of 1:2 was gradually introduced to the mixture while stirring continuously for 5 h. The mixture was then subjected to 200W ultrasonication for 2 h at 50°C. The resulting pale-yellow solution was centrifuged and dried at 100°C. A similar procedure was used to synthesize $AgIO_4$ but excluding $SrTiO_3$.

FESEM and EDX mapping were performed using a JEOL JSM-6701 F FESEM paired with an Oxford X-Max 20 EDX system. The crystalline structure of as-synthesized samples was examined via a Philips PW1820 X-ray diffractometer with a scanning range of 10–80° at λ = 0.15406 nm. FTIR analysis was carried out using a Perkin Elmer Spectrum Two™ FTIR Spectrometer at scanning spectral from 400-4000 cm^{-1}. UV-vis DRS of samples was performed by a Perkin Elmer Lambda 35 UV–vis spectrometer. Photoelectrochemical measurements including EIS and TPR were conducted using a Gamry Interface 1000T potentiostat electrochemical workstation, employing Ag/AgCl, as-prepared samples and Pt wire as the reference, working and counter electrodes, respectively.

For photocatalysis, CFX solution (80 mL, 20 mg/L) was stirred with prepared photocatalyst (40 mg) in darkness for 30 min to achieve equilibrium. A 150 W LED lamp was utilized as the simulated solar light source. During irradiation, the extracted CFX solution was tested using UV-vis spectrophotometer. The degradation performance was calculated via equation $(C_o–C_t)/C_o$, where C_o represents equilibrium CFX concentration and C_t is the concentration at time t.

3 Results and discussion

3.1 Morphological analysis

FESEM was employed to scrutinize the morphological features of samples, as shown in Figure 1. $SrTiO_3$ exhibited hierarchical flower-like microspheres composed of interconnecting nanosheets [Figure 1(a)]. $AgIO_4$ nanoparticles appeared in both bulk and agglomerated states, with sizes ranging from 100-200 nm [Figure 1(b)]. Figure 1(c) showed that the $AgIO_4$ nanoparticles were uniformly dispersed over the $SrTiO_3$ microspheres as well as completely encapsulating the flower-like structures, which demonstrated the successful synthesis of $SrTiO_3/AgIO_4$ heterostructure. Moreover, the EDX mapping in Figure 1(d) confirmed the homogeneous distribution of Ti, Sr, O, I and Ag elements on $SrTiO_3/AgIO_4$ composite.

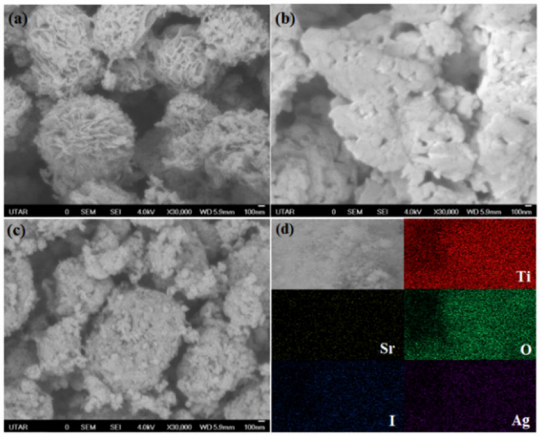

Fig. 1. FESEM images of (a) $SrTiO_3$, (b) $AgIO_4$ and (c) $SrTiO_3/AgIO_4$. (d) EDX mapping of $SrTiO_3/AgIO_4$ composite.

3.2 Structural and compositional characterization

Figure 2(a) shows the XRD patterns of $SrTiO_3$, $AgIO_4$ and the $SrTiO_3/AgIO_4$ composite. The

$SrTiO_3$ displayed a cubic perovskite structure, matching perfectly with JCPDS no. 35-0734, whereas $AgIO_4$ presented an orthorhombic structure as per JCPDS no. 01-071-3844 [8-9]. The diffraction peaks for the $SrTiO_3/AgIO_4$ composite clearly demonstrated the coexistence of both phases without impurities, indicating the successful formation of a Z-scheme heterostructure. The FTIR spectra of as-prepared samples are shown in Figure 2(b). The peaks observed at 856 and 574 cm^{-1} were ascribed to the Sr-O and Ti-O bond stretching, respectively [6,10]. The peaks at 569 cm^{-1} and 768 cm^{-1} were symbolizing the stretching vibrations of the Ag-I bond [11]. The bands at 1611 cm^{-1} and 3406 cm^{-1} across all spectra were due to adsorbed water [12]. The presence of all characteristic absorption bands in the spectra of the $SrTiO_3/AgIO_4$ composite further confirmed the successful synthesis of the heterostructure.

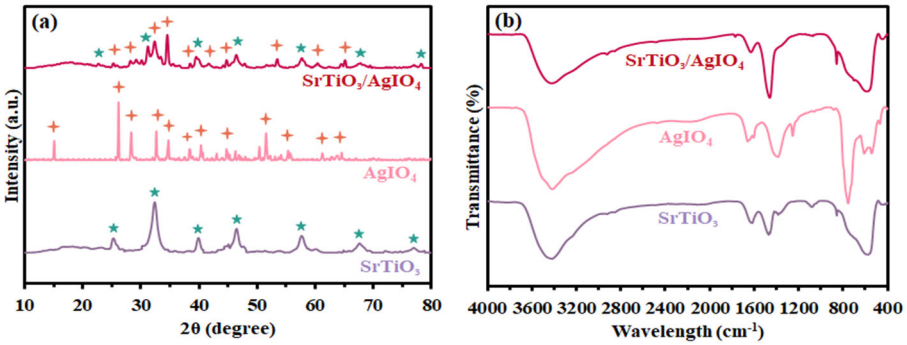

Fig. 2. (a) XRD patterns and (b) FTIR spectra of as-synthesized samples.

3.3 Photocatalytic Activity and Mechanism

The spectral changes of CFX over irradiation time in Figure 3(a) revealed a progressive decrease in characteristic absorption peaks, indicating successful photodegradation of CFX over $SrTiO_3/AgIO_4$. The photodegradation of CFX over different photocatalysts is illustrated in Figure 3(b). Dark test and photolysis showed minimal degradation, highlighting CFX degradation were performed at an almost pure photocatalytic condition. Interestingly, the $SrTiO_3/AgIO_4$ composite achieved 73.8% degradation within 120 min, vastly surpassing the individual performances of $SrTiO_3$ (5.7%) and $AgIO_4$ (51.9%). Meanwhile, the physical mixture of $SrTiO_3$ and $AgIO_4$ ($SrTiO_3/AgIO_4$-mix) only managed to degrade 55.7% of CFX. This contrast underscored the significant role of the heterojunction structure in $SrTiO_3/AgIO_4$, which enhanced interfacial charge transfer and thereby boosting photocatalytic activity. Similar findings have also been reported by Kokilavani et al. [8] and Wang et al. [10] on their superior performance of composite compared to single components. Their photocatalytic improvement was credited to the formation of heterojunction nanocomposite resulting in the charge migrating between the photoexcited individual semiconductor. Furthermore, the corresponding rate constants were obtained by fitting the pseudo-first-order kinetic model [Figure 3(c)]. The kinetic rate constants of $SrTiO_3$, $AgIO_4$, $SrTiO_3/AgIO_4$-mix and $SrTiO_3/AgIO_4$ were 0.0005, 0.0065, 0.0072 and 0.0113 min^{-1}, respectively. Prominently, the $SrTiO_3/AgIO_4$ composite exhibited a degradation rate constant that was 22-folds higher than that of $SrTiO_3$ alone and nearly 1.7-folds of $AgIO_4$.

From Figure 3(d-e), both the transient photocurrent response and Nyquist plots displayed that the electron-hole pair separation and charge transfer efficiency followed the order of $SrTiO_3/AgIO_4 > AgIO_4 > SrTiO_3$, which implied the significance of Z-scheme heterostructure in improving photoelectronic performance. Furthermore, the band gap energy values were estimated by performing a linear extrapolation of $(\alpha hv)^2$ vs. hv plots [Figure 3(f)]. The band

gap energies (E_g) for $SrTiO_3$, $AgIO_4$ and the $SrTiO_3/AgIO_4$ were observed to be 3.05, 2.25 and 2.98 eV, respectively. The valence band (VB) and conduction band (CB) edge potentials of a semiconductor are calculated using the formulas: $E_{VB} = X - E_e + 0.5E_g$ and $E_{CB} = E_{VB} - E_g$, where E_e denotes the free electrons energy (4.5 eV) and X represents the absolute electronegativity (X values for $SrTiO_3$ and $AgIO_4$ are 4.95 eV and 6.78 eV, respectively) [13]. Therefore, the E_{VB} are 1.98 eV for $SrTiO_3$ and 3.41 eV for $AgIO_4$. Correspondingly, the E_{CB} are -1.07 eV for $SrTiO_3$ and 1.16 eV for $AgIO_4$.

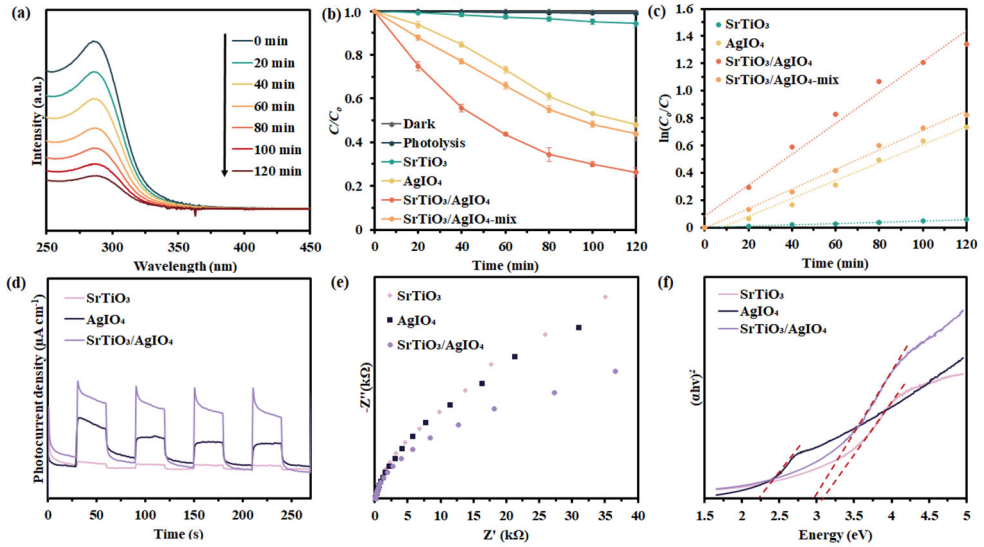

Fig. 3. (a) Spectral changes of CFX versus irradiation time over $SrTiO_3/AgIO_4$, (b) CFX degradation and (c) corresponding kinetic curve. (d) TPR, (e) EIS and (f) Tauc plot of as-synthesized samples.

Based on the results obtained, an enhanced photocatalytic degradation of CFX has been explained through the proposed Z-scheme heterojunction mechanism, as depicted in Figure 4. Under light irradiation, both $SrTiO_3$ and $AgIO_4$ generated electron-hole pairs, where the electrons from the lower conduction band energy of $AgIO_4$ moved to $SrTiO_3$ and recombined with its holes in the valence band, effectively suppressing recombination in both semiconductors. The remaining electrons in conduction band of $SrTiO_3$, with more negative potential than $O_2/\bullet O_2^-$ (−0.33 eV vs NHE) reduced adsorbed O_2 to form $\bullet O_2^-$ radicals [14]. Conversely, holes in the valence band of $AgIO_4$, which were more positive than both $OH^-/\bullet OH$ (2.38 eV vs NHE) and $H_2O/\bullet OH$ (2.72 eV vs NHE) oxidized water or hydroxide ions to produce •OH radicals [15]. These highly oxidizing reactive species then engaged actively to degrade CFX. Thus, this Z-scheme heterojunction promoted effective charge carrier separation and exhibited robust redox capabilities thereby enhancing the photocatalytic efficiency of $SrTiO_3/AgIO_4$.

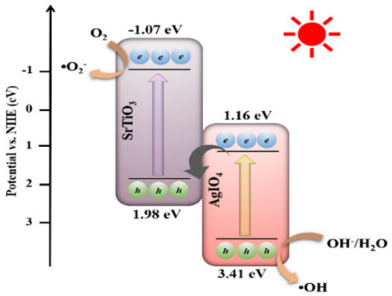

Fig. 4. Z-scheme heterojunction mechanism over $SrTiO_3/AgIO_4$ composite.

4 Conclusion

In closing, this research successfully synthesized $SrTiO_3/AgIO_4$ composite using a facile surfactant-free solvothermal-sonochemical route. Various analytical methods verified the creation of a heterojunction between $SrTiO_3$ and $AgIO_4$. Photocatalytic assessments showed that the $SrTiO_3/AgIO_4$ composite exhibited outstanding photoactivity in degrading CFX under simulated sunlight. The elevated performance was attributed to the Z-scheme heterojunction mechanism, which promoted efficient charge carrier separation and high redox potential for boosted photocatalytic activity. The results unveiled the potential of Z-scheme heterojunctions in advancing photocatalysts for environmental applications, inspiring future research to delve into scalability, stability, and broader pollutant remediation.

This research was supported by Ministry of Higher Education, Malaysia (MoHE) through Fundamental Research Grant Scheme (FRGS/1/2022/TK08/UTAR/02/5). The authors also thank to the Research funds of The Guangxi Key Laboratory of Theory and Technology for Environmental Pollution Control, China (1801K012 and 1801K013), ASEAN Young Talented Scientist Program of Guangxi, China (DT2200002995 and DT2200002996) and special funding for "Guangxi “Bagui Scholar” Construction Project, China".

References

1. S. Arabian, A. Gordanshekan, M. Farhadian, A. R. S. Nazar, S. Tangestaninejad, H. Sabzyan, Adsorption/photocatalytic degradation of cefixime by the green Bi_2WO_6/g-C_3N_4/ZIF-67 dual S-scheme heterojunction: Artificial neural network, genetic algorithm, density functional theory, and toxicity assessments. Chem. Eng. J. **488**, 150686 (2024). https://doi.org/10.1016/j.cej.2024.150686
2. B. Harikumar, S. Kokilavani, S. S. Khan, Magnetically separable N/S doped Fe_3O_4 embedded on MoO_3 nanorods for photodegradation of cefixime, Cr(VI) reduction, and its genotoxicity study. Chem. Eng. J. **446**, 137273 (2022). https://doi.org/10.1016/j.cej.2022.137273
3. C. Li, H. Che, Y. Yan, C. Liu, H. Dong, Z-scheme $AgVO_3/ZnIn_2S_4$ photocatalysts: “One Stone and Two Birds” strategy to solve photocorrosion and improve the photocatalytic activity and stability. Chem. Eng. J. **398**, 125523 (2020). https://doi.org/10.1016/j.cej.2020.125523
4. Z. He, H. Yang, J. Su, Y. Xia, X. Fu, L. Wang, L. Kang, Construction of multifunctional dual Z-scheme composites with enhanced photocatalytic activities for degradation of ciprofloxacin. Fuel. **294**, 120399 (2021). https://doi.org/10.1016/j.fuel.2021.120399
5. G. Venkatesh, P. Shobana, N. Elavarasan, A. Rajesh, S. Senthilnathan, V. Vignesh, Rational strategy for the construction of Z-scheme based MoS_2/Co_3O_4 coupled $SrTiO_3$ nanocomposite for dye degradation: An experimental and theoretical insights. Mater. Sci. Semicond. Process. **169**, 107909 (2024). https://doi.org/10.1016/j.mssp.2023.107909
6. M. Sohrabian, V. Mahdikhah, E. Alimohammadi, S. Sheibani, Improved photocatalytic performance of $SrTiO_3$ through a Z-scheme polymeric-perovskite heterojunction with g-C_3N_4 and plasmonic resonance of Ag mediator. Appl. Surf. Sci. **618**, 156682 (2023). https://doi.org/10.1016/j.apsusc.2023.156682
7. A. Kumar, S. K. Sharma, A. Kumar, G. Sharma, N. AlMasoud, T. S. Alomar, M. Naushad, Z. A. Alothman, F. J. Stadler, High interfacial charge carrier separation in Fe_3O_4 modified $SrTiO_3/Bi_4O_5I_2$ robust magnetic nano-heterojunction for rapid

photodegradation of diclofenac under simulated solar-light. J. Clean. Prod. **315**, 128137 (2021). https://doi.org/10.1016/j.jclepro.2021.128137

8. S. Kokilavani, A. Syed, A. M. Elgorban, A. H. Bahkali, H. A. Al-Shwaiman, R. S. Varma, A. Das, S. Khan, Designing Z-scheme $AgIO_4$ nanorod embedded with Bi_2S_3 nanoflakes for expeditious visible light photodegradation of congo red and rhodamine B. Chemosphere. **294**, 133755 (2022). https://doi.org/10.1016/j.chemosphere.2022.133755
9. X. Yu, J. Wang, X. Fu, H. Meng, Y. Zhu, Y. Zhang, Construction of Z-scheme $SrTiO_3$/Ag/Ag_3PO_4 photocatalyst with oxygen vacancies for highly efficient degradation activity towards tetracycline. Sep. Purif. Technol. **241**, 116718 (2020). https://doi.org/10.1016/j.seppur.2020.116718
10. X. Wang, L. Jiang, K. Li, J. Wang, D. Fang, Y. Zhang, D. Tian, Z. Zhang, D. D. Dionysiou, Fabrication of novel Z-scheme $SrTiO_3$/$MnFe_2O_4$ system with double-response activity for simultaneous microwave-induced and photocatalytic degradation of tetracycline and mechanism insight. Chem. Eng. J. **400**, 125981 (2020). https://doi.org/10.1016/j.cej.2020.125981
11. R. Abdel-Aziz, M. Ahmed, M. F. Abdel-Messih, A novel UV and visible light driven photocatalyst $AgIO_4$/ZnO nanoparticles with highly enhanced photocatalytic performance for removal of rhodamine B and indigo carmine dyes. J. Photochem. Photobiol. A. **389**, 112245 (2020). https://doi.org/10.1016/j.jphotochem.2019.112245
12. Y. Jia, H. Han, Y. Luo, Q. Wang, B. W. Lee, C. Liu, $SrTiO_3$ nanosheets decorated with $ZnFe_2O_4$ nanoparticles as Z-scheme photocatalysts for highly efficient photocatalytic degradation and CO_2 conversion. Sep. Purif. Technol. **306**, 122667 (2023). https://doi.org/10.1016/j.seppur.2022.122667
13. N. Askari, M. Beheshti, D. Mowla, M. Farhadian, Facile construction of novel Z-scheme $MnWO_4$/Bi_2S_3 heterojunction with enhanced photocatalytic degradation of antibiotics. Mater. Sci. Semicond. Process. **127**, 105723 (2021). https://doi.org/10.1016/j.mssp.2021.105723
14. Y. Wang, C. Zhu, G. Zuo, Y. Guo, W. Xiao, Y. Dai, J. Kong, X. Xu, Y. Zhou, A. Xie, C. Sun, Q. Xian, 0D/2D Co_3O_4/TiO_2 Z-Scheme heterojunction for boosted photocatalytic degradation and mechanism investigation. Appl. Cat. B. Environ. **278**, 119298 (2020). https://doi.org/10.1016/j.apcatb.2020.119298
15. J. Sin, S. Lam, H. Zeng, H. Lin, H. Li, A. K. Kumaresan, A. R. Mohamed, J. Lim, Z-scheme heterojunction nanocomposite fabricated by decorating magnetic $MnFe_2O_4$ nanoparticles on BiOBr nanosheets for enhanced visible light photocatalytic degradation of 2,4-dichlorophenoxyacetic acid and Rhodamine B. Sep. Purif. Technol. **250**, 117186 (2020). https://doi.org/10.1016/j.seppur.2020.117186